Journal of Visualized Experiments

An In Vitro Single-Molecule Imaging Assay for Analysis of Cap-Dependent Translation Kinetics

--Manuscript Draft--

Article Type:	Invited Methods Article - JoVE Produced Video
Manuscript Number:	JoVE61648R2
Full Title:	An In Vitro Single-Molecule Imaging Assay for Analysis of Cap-Dependent Translation Kinetics
Corresponding Author:	Xiaohui Qu Memorial Sloan Kettering Cancer Center New York, NY UNITED STATES
Corresponding Author's Institution:	Memorial Sloan Kettering Cancer Center
Corresponding Author E-Mail:	qux@mskcc.org
Order of Authors:	Anthony Gaba
	Hongyun Wang
	Xiaohui Qu
Additional Information:	
Question	**Response**
Please indicate whether this article will be Standard Access or Open Access.	Standard Access (US$2,400)
Please indicate the **city, state/province, and country** where this article will be **filmed**. Please do not use abbreviations.	New York, NY, USA 10065

TITLE

An In Vitro Single-Molecule Imaging Assay for the Analysis of Cap-Dependent Translation Kinetics

AUTHORS AND AFFILIATIONS

Anthony Gaba[1*], Hongyun Wang[1*], Xiaohui Qu[1]

[1] Molecular Biology Program, Memorial Sloan Kettering Cancer Center, New York, New York, USA

*These authors contributed equally to this paper.

Email addresses of coauthors:
Anthony Gaba (gabaa@mskcc.org)
Hongyun Wang (wangh4@mskcc.org)

Corresponding author:
Xiaohui Qu (qux@mskcc.org)

KEYWORDS:

cell-free eukaryotic translation, single-molecule translation kinetics, in vitro fluorescence imaging, cap-dependent initiation, translational control, in vitro assay

SUMMARY:

Tracking individual translation events allows for high-resolution kinetic studies of cap-dependent translation mechanisms. Here we demonstrate an in vitro single-molecule assay based on imaging interactions between fluorescently labeled antibodies and epitope-tagged nascent peptides. This method enables single-molecule characterization of initiation and peptide elongation kinetics during active in vitro cap-dependent translation.

ABSTRACT:

Cap-dependent protein synthesis is the predominant translation pathway in eukaryotic cells. While various biochemical and genetic approaches have allowed extensive studies of cap-dependent translation and its regulation, high resolution kinetic characterization of this translation pathway is still lacking. Recently, we developed an in vitro assay to measure cap-dependent translation kinetics with single-molecule resolution. The assay is based on fluorescently labeled antibody binding to nascent epitope-tagged polypeptide. By imaging the binding and dissociation of antibodies to and from nascent peptide–ribosome–mRNA complexes, the translation progression on individual mRNAs can be tracked. Here, we present a protocol for establishing this assay, including mRNA and PEGylated slide preparations, real-time imaging of translation, and analysis of single molecule trajectories. This assay enables tracking of individual cap-dependent translation events and resolves key translation kinetics, such as initiation and elongation rates. The assay can be widely applied to distinct translation systems and should broadly benefit in vitro studies of cap-dependent translation kinetics and

translational control mechanisms.

INTRODUCTION:

Translation in eukaryotic systems occurs predominantly through 7-methylguanosine cap-dependent pathways[1]. Studies indicate that the initiation step of eukaryotic translation is rate-limiting and a common target for regulation[2-4]. Mechanisms of cap-dependent translation have been extensively studied using genetic[5], biochemical[6-8], structural[9], and genomic[10] bulk approaches. Although these methods have identified diverse mechanisms that regulate cap-dependent initiation, their resolution limits them to ensemble averaging of signals from heterogeneous and asynchronous initiation events. More recently, individual in vivo translation events have been visualized by methods that measure fluorescent antibody binding to epitopes on nascent polypeptides[11-14]. However, these new approaches are also limited in their ability to resolve individual initiation events because multiple fluorescent antibodies must bind a nascent peptide to allow single translation events to be resolved from a high intracellular fluorescence background. In many biological interactions, resolved individual kinetic events have provided critical insights into understanding complex multistep and repetitive biological processes that are not possible to synchronize at the molecular level. New methods that can track the dynamics of individual translation events are needed for a better understanding of cap-dependent initiation and regulation.

We recently developed an in vitro assay that measures cap-dependent initiation kinetics with single-molecule resolution[15]. Considering the large number of known and unknown protein factors involved in this initiation pathway[3,16], the single-molecule assay was developed to be compatible with existing in vitro cell-free translation systems to benefit from their preservation of cellular factors and robust translation activity[17-25]. Furthermore, the use of cell-free translation systems allows more compatible comparisons between single-molecule observations and previous bulk results. This approach provides a straight-forward integration of new single-molecule kinetic insights into the existing mechanistic framework of cap-dependent initiation. To establish the single-molecule assay, the traditional cell-free translation system is modified in three ways: an epitope-encoding sequence is inserted at the beginning of the open reading frame (ORF) of a reporter mRNA; the 3′ end of the reporter mRNA is biotinylated to facilitate mRNA end-tethering to single-molecule detection surface; and fluorescently-labeled antibodies are supplemented to the translation extract. These modifications require only basic molecular biology techniques and commonly available reagents. Furthermore, these modifications and the single-molecule imaging conditions preserve the translation kinetics of bulk cell-free translation reactions[15].

In this assay (**Figure 1**), 5′-end capped and 3′-end biotinylated reporter mRNA is immobilized to a streptavidin-coated detection surface in a flow chamber. The flow chamber is then filled with a cell-free translation mixture supplemented with fluorescently labeled antibodies. After mRNA translation has occurred for approximately 30-40 codons downstream of the epitope sequence[26,27], the epitope emerges from the ribosome exit tunnel and becomes accessible to interact with fluorescently-labeled antibody. This interaction is rapid and its detection by single-molecule fluorescence imaging techniques enables tracking of translation kinetics with single-

molecule resolution during active cell-free translation. This assay should broadly benefit in vitro studies of cap-dependent translation kinetics and its regulation, particularly for systems with a working bulk in vitro assay.

A prerequisite for establishing this single-molecule assay is a working bulk cell-free translation assay, which can be achieved using translation extract that is either commercially available or prepared following previously described methods[28]. Eukaryotic translation extract can be obtained from diverse cells, including fungal, mammalian, and plant[28]. For imaging, this assay requires a TIRF microscope equipped with tunable laser intensity and incident angle, a motorized sample stage, a motorized fluidics system, and sample temperature control device. Such requirements are generic for modern in vitro single-molecule TIRF experiments and may be achieved differently. The experiment presented here uses an objective-type TIRF system made up of commercially available microscope, software, and accessories all listed in the **Table of Materials**.

PROTOCOL:

1. Generation of reporter mRNA

1.1. Modify a DNA transcription template that encodes a bulk-assay "untagged" reporter mRNA by inserting an N-terminus epitope tag-encoding sequence to generate a DNA transcription template for a "tagged" reporter mRNA (**Figure 2A**).

NOTE: 3xFLAG/anti-FLAG interaction is recommended for this assay due to its superior sensitivity and the short 3xFLAG tag length. However, the assay is compatible with other epitope/antibody pairs.

1.2. Synthesize untagged and tagged RNAs using linearized DNA templates and an in vitro transcription kit (see **Table of Materials**). Typically, 10–20 pmol of in vitro transcribed RNA is sufficient for subsequent RNA processing to allow a systematic single-molecule study.

1.3. Cap the RNA 5′ end (**Figure 2B**) with an m^7G capping kit (see **Table of Materials**) following the manufacturer's recommendation.

1.4. Biotinylate the RNA 3′ end (**Figure 2B**) using a biotinylation kit (see **Table of Materials**) as per the protocol provided with the kit. Purify RNAs by phenol-chloroform extraction followed by purification with a spin column. Elute RNA in 10–20 μL of RNase-free water. Approximately 40–50% of the uncapped input RNA is recovered.

1.6. Assess RNA integrity and concentration by denaturing acrylamide gel electrophoresis and RNA staining, as described previously[29].

1.7. Perform bulk cell-free translation[30] with the 3′-end-biotinylated tagged reporter mRNA to confirm that the modified mRNA preserves the translation properties that are of interest. As an

example, cap-dependent translation can be confirmed by measuring and comparing reporter activities in bulk cell-free translation reactions with uncapped and capped reporter mRNAs (see **Representative Results**).

2. Flow chamber preparation

2.1. Select an appropriate coverslip thickness, as specified by the microscope objective spec sheet. Select a glass or quartz slide for objective- or prism-type total internal reflection fluorescence (TIRF) imaging systems[31], respectively.

2.2. Perform cleaning, salinization, PEGylation, and chamber assembly of coverslip and slides following the protocol described by Chandradoss et al.[32] with the following modifications.

2.2.1. Wash slides containing drilled holes in 10% alkaline liquid detergent (v/v) for 20 min with sonication. Combine the slides and coverslips for all remaining cleaning steps.

2.2.2. Skip the acetone wash step. Extend the Piranha etching incubation time from 20 min to 1 h. Incubate the first-round PEGylation for 3 h. Incubate the second-round PEGylation with MS(PEG)4 for 3 h.

3. Equipment preparation

3.1. At least 3 h before performing a single-molecule experiment, turn on the microscope incubator and reduce the airflow to a low rate to avoid excessive acoustic disturbance of experiments. Set the incubator temperature to the optimal temperature for the cell-free translation system.

NOTE: Translation is extremely sensitive to temperature. The optimal reaction temperature is specific for each cell extract system. Reaction temperature characterization is a vital step in the development of a bulk cell-free translation system. This single-molecule assay should be conducted under the same optimal temperature as the corresponding bulk translation condition.

3.2. At least 1 h before performing a single-molecule experiment turn the laser on by pressing the laser power button behind the laser box, turn the laser safety key, and press the start button; turn on the microscope and tap on the touch screen control panel to select the imaging mode, objective, and filter set.

3.3. Turn on the EMCCD camera, the Prior stage controller, and the syringe pump by pressing their power buttons. Turn on the computer and open software *Andor Solis* (software 1) to control the EMCCD camera, *TirfCtrl* (software 2) to control the laser, *PriorTest* (software 3) to control the motorized stage, and *Coolterm* to control the syringe pump. Allow the camera to cool and stabilize to its designated working temperature before data acquisition begins.

3.4. In software 2, confirm that the correct parameters are set for laser wavelength, objective type, and refractive index of glass and sample. Click the **Connect** button and to set the laser intensity, click the **Control** button next to the laser wavelength, then in the laser control pop up window, drag the intensity slide bar. Set the laser to the desired angle by dragging the fiber position slide bar or inputting the corresponding penetration depth. Ensure that the **Shutter box** is checked to maintain the laser in the **Off mode** when not imaging.

NOTE: Open and close the laser shutter by checking the **Shutter** box. When initially establishing the assay, different laser intensities and incident angles should be tested for optimal single-molecule detection. The optimal laser intensity balances bright single-molecule fluorescence and fast photobleaching of the fluorophores. The incident angle should be increased beyond the critical angle to reduce the high fluorescent background from the diffusing labeled antibodies until mRNA-bound antibodies are clearly resolved. As a reference, a 532 nm laser was set to 10 μW at the objective with the laser incident angle set to 71.5° in a study[15] using Cy3-labeled anti-FLAG with a labeling ratio of 2–7 dyes per antibody.

3.5. In software 1, choose **Kinetic** under the **Acquisition Mode**, input the parameters for exposure time, kinetic series length, and EM gain value. Choose the directory and assign filenames for saving the data image file.

3.6. Set the syringe pump to a modest to fast flow rate for the subsequent tubing washing step. Pipette an aliquot of 70% ethanol into a microfuge tube, insert the syringe pump tubing end into the ethanol solution, and use *Coolterm* to toggle the syringe pump between withdraw and dispense modes three times to wash the tubing. Repeat using RNase-free water.

NOTE: The tubing length must be long enough to allow the translation mix to be dispensed at step 5 to only contact the tubing, not the syringe. The rinse volume here should be greater than the volume of dispensed translation mix to ensure that the translation mix at step 5 remains in contact with sanitized tubing.

3.7. After the final water rinse has been dispensed, remove residual water from the inside of the tubing by dabbing the tubing end on a clean tissue wipe. Maintain the tubing end dry by setting it into a clean microfuge tube.

4. Immobilization of 3′-end biotinylated mRNA

4.1. Maintain the cell extract and translation mix frozen on dry ice until just before their use. Thaw the remaining frozen reagents and maintain them on ice.

4.2. Place the flow chamber into the microscope sample holder with the coverslip side facing down and secure it in place with tape. Use tape to cover the inlets and outlets of flow channels that are not in use.

4.3. Pipette a 1.5x volume (relative to channel volume; also applies to other steps in step 4 and

step 5) of 0.2 mg/mL streptavidin into the flow channel and incubate for 10 min at room temperature.

4.4. To remove unbound streptavidin, wash the channel three times by pipetting in a 3x volume of T50 wash buffer (20 mM Tris HCl, pH 7.0, 50 mM NaCl, 0.2 U/μL RNase inhibition reagent) per wash.

NOTE: It is important to prevent liquid waste from flowing back into the channel. If the outlet of the flow channel is not connected to a waste collection tube, place a folded tissue paper near the outlet to absorb the liquid that flows out of the channel.

4.5 Transfer the translation extract and mix from dry ice to ice and allow them to thaw.

4.6. Put a drop of immersion oil on the objective. Place the microscope sample holder with the flow chamber into the microscope stage. Bring the objective close to the coverslip until immersion oil on the objective contacts the coverslip. Move the sample stage so that the position of the flow channel is directly above the objective lens.

4.7. In software 2, open the laser shutter and adjust the laser intensity level

4.8. On the microscope control touch screen, select the **Focus** tab and click the **Focus Search** and **Start** button. A beep is heard when a focus plane is successfully achieved.

4.9. Image the flow channel surface in **Live** mode in software 1. Optimize the focus for a sharper image by adjusting the objective position with the fine step control on the touch screen.

4.10. In software 3, move the stage to evaluate the level of fluorescence background at various areas of the flow channel detection surface. If the fluorescence is low, continue with the experiment. If the fluorescence background is excessively high, consider discarding the flow channel.

4.11. In software 2, close the laser shutter.

4.12. Pipette out the T50 wash buffer from the flow channel and immediately pipette in a 2x volume of biotinylated mRNA solution to the flow channel. Incubate for 15 min.

NOTE: For each batch of mRNA preparation, mRNA concentrations and incubation times should be tested to achieve the mRNA surface density necessary for single-molecule detection. Appropriate mRNA surface density mediates antibody binding that shows fluorescent spots with no more than ~5% overlapping (see **Representative Results**). As a starting point, biotinylated mRNA at a concentration of 2–20 nM is recommended.

4.13. Wash the channel three times by pipetting a 3x volume of translation compatible buffer

per wash.

5. Translation mix assembly and delivery to a flow channel for single-molecule detection

5.1. On ice, assemble 3x volumes of the translation mix[30] in a microcentrifuge tube following the bulk translation protocol from step 1.7, except omit mRNA and supplement with an optimized concentration of fluorescently labeled antibodies. Briefly spin the microcentrifuge tube to collect the translation mix at the bottom of the tube.

NOTE: When establishing the assay, different antibody concentrations are tested. The optimal concentration shows low amounts of nonspecific antibody binding to the detection surface and fast antibody binding to the nascent peptide (see steps 7.1. and 7.2., respectively, for assay calibration details).

5.2. Transfer the translation mix to the inside of a 0.7 mL microfuge tube cap. Set the syringe pump to the withdraw mode. Insert the pump tubing end into the translation mix. Start the syringe withdrawal to collect the translation mix into the pump tubing. Reverse the syringe pump setting to the dispensing mode and set the flow to an optimal rate for translation mix delivery.

NOTE: Avoid generating bubbles in the translation mix when transferring it into the pump tubing. Avoid withdrawing the translation mix too deep into the part of the tubing that was not sanitized and rinsed in step 3.6. When establishing the assay, different delivery flow rates are tested to determine the optimal rate (see step 6.2. for details on assay calibration).

5.3. If there is a gap between the tubing end and translation mixture, start the syringe pump and allow the translation mixture to reach the tubing end, then stop the syringe pump.

5.4. Insert the pump tubing end into the inlet of the flow channel. Avoid introducing air bubbles into the translation mix when performing the connection. Stabilize the connection by screwing the custom-made metal bracket onto the microscope sample holder plate. Assess the microscope focus and imaging area fluorescence.

NOTE: The tubing can be clamped to the flow chamber with a custom part as previously described[33]. Other types of fluidics system can also be used for this assay[34]. The field of view should appear similar before and after connecting the tubing. If more fluorescent spots appear after the connection, the translation mix is likely leaking from the delivery tubing. Depending on the application, the channel with leaked translation mix may need to be discarded.

5.5. Confirm that the movie acquisition parameters are correct and that the appropriate filename and directory have been entered for saving files.

5.6. Move the stage to image an area in the center of the flow channel detection surface. On the microscope control touch screen, select the **Continuous AF** tab and click the **Focus Search**

and **Start** button to maintain the focal position during the experiment. A beep is heard when a focus plane is successfully achieved.

5.7. In software 2, open the laser shutter. In software 1, click the **Take Signal** button to start recording. After approximately 5 s of recording, enter the **Run** command in *Coolterm* to deliver the translation mix into the flow channel. Record for up to 2 h with a time resolution of 0.5–2 s/frame.

NOTE: The maximum span of data acquisition depends on how fast the translation extract loses activity over time, which can be conveniently characterized by performing bulk cell-free translation with luciferase reporter mRNA and measuring luciferase activity in the translation reactions at different time points[35].

5.8. When data acquisition is complete, turn off the laser, turn off the **Continuous AF** on the microscope control touch screen, and disassemble the tubing from the flow chamber.

5.9. Pipette out the translation mixture from the flow channel inlet, transfer it to a microfuge tube, and snap-freeze the solution by placing the tube in liquid nitrogen. Later store at -80 °C.

5.10. Wash the syringe pump tubing three times with RNase-free water, then three times with 70% ethanol. Withdraw 70% ethanol into the syringe pump tubing for storage.

5.11. Turn off the microscope and all accessories. Clean up.

6. Data analysis

NOTE: Data analysis for this assay requires common methods in single-molecule biophysical studies. All computationally intensive steps can be achieved using existing algorithms and software (references are included below at their corresponding steps).

6.1. Optional: If applicable, convert the acquired image series file to a format that is compatible with the chosen image processing software or programming language.

6.2. Determine the translation reaction starting point and reagent exchange time.

NOTE: Due to the diffusing fluorescent antibodies in the translation mix, the background fluorescence intensity of an imaged area will increase during the in-channel reagent exchange from translation compatible buffer to translation mix. The translation reaction starting point is set as the time point when the reagent exchange is complete. This completion point is found by measuring the background fluorescence intensity during the translation mix delivery and identifying the time point when the increasing fluorescence intensity plateaus[15], as described below.

6.2.1. Calculate the total fluorescence counts per image frame and plot the corresponding time

profile. Identify the sudden increase in total fluorescence in the time profile plot.

NOTE: The total fluorescence increase is due to the increasing concentration of fluorescently labeled antibody during the reagent exchange.

6.2.2. Identify the end point of the total fluorescence increase phase and set this time point as the starting point (i.e., time 0) of the translation reaction. Identify both the start and end points of the total fluorescence increase phase and set the time difference as the reagent exchange time.

NOTE: The total time-span of reagent exchange depends on the flow channel dimensions and the selected flow rate. It is possible that some translation factors can start binding to mRNA before the reagent exchange completes, which could reduce the resolution of the determined first-round initiation time. It is therefore recommended to test different flow rates when setting up the assay and select flow rates that allow reagent exchange completion within 3–4 s for data acquisition speeds of 0.5–2 s/frame.

6.3. Optional: Perform movie drift correction.

NOTE: The positions of bound antibodies in the data image might change over time due to drift of microscope parts and accessories. Drift that is visually noticeable in a movie requires correction before proceeding further with data analysis. Several spatial drift correction algorithms and scripts are available[36-38].

6.3.1. In each image, find the local maxima in pixel counts to determine the positions of bound antibodies in each frame with pixel-level accuracy. Set a threshold of the pixel count such that only spots that are clearly above the background noise are selected.

6.3.2. Calculate the changes of individual antibody positions in each direction between two consecutive image frames.

6.3.3. Plot the histogram of antibody positional changes between two consecutive frames and do so separately for each direction. Gaussian fit each histogram and set the center position of peaks as the directional drift between two consecutive frames.

6.3.4. To counteract the observed drift, shift each image frame in the opposite direction by the calculated drift amount.

6.4. Construct single-molecule trajectories.

NOTE: Detection/tracking software is available to identify bright spots and extract their intensities from data image series[39,40].

6.4.1. Identify antibody positions as described in step 6.3.1.

NOTE: Visual inspection is recommended to ensure that the chosen threshold does not give rise to excessive over- or under-picking of particles. Visual inspection can be achieved by overlaying the identified centroid positions over each image frame and visually assessing their agreement (see **Representative Results**).

6.4.2. Combine the picked particles from all frames and remove the redundant particle positions.

6.4.3. Visually inspect the images of bound antibodies and select a square area enclosing the pixels with counts that are clearly above background and representative of individually bound antibody.

NOTE: The point spread function (i.e., the size of the square for a single molecule) is determined by the optical setup and the detector pixel size.

6.4.4. For each particle position, construct a single-molecule trajectory by calculating the total intensity of all pixels in the square area around the particle position. Trajectories are constructed for each position, frame by frame, and for the whole data movie.

6.5. Optional: Apply a non-linear forward-backward filter[41] to reduce background noise in single-molecule trajectories.

6.6. Optional: Digitize trajectories with existing step-detection algorithms[42-45].

NOTE: The choice of step-detection algorithm depends on the complexity of the single-molecule dynamics. For the simplest scenario of only isolated ribosome translation (i.e. no polysome formation) and good signal to noise ratio, a threshold application to the fluorescence counts is sufficient for identifying the timing of antibody binding and dissociation events in the single-molecule trajectories. Visual inspection of at least 100 trajectories for each condition is recommended to ensure that trajectory steps have been appropriately selected by a step-detection strategy.

6.7. Determine the time of the first antibody binding event for each trajectory (i.e., first arrival time, t_1), either using digitized trajectories or applying a threshold to undigitized trajectories.

NOTE: The median value of the first arrival time distribution can be compared between different translation conditions. Alternatively, the first arrival time distribution can be fitted to a shifted (3-parameter) log-normal function to determine the mean value[15] $\langle t_1 \rangle$. Because the first arrival time distribution is typically skewed and has a long tail, do not calculate the mean by directly averaging over the observed first arrival times.

6.8. Optional: Dwell time analysis and calculation of average peptide synthesis rate.

6.8.1. Use digitized trajectories to identify monosome (single ribosome) translation events in each trajectory and calculate the single binding event dwell times as the time difference between corresponding antibody binding and dissociation events.

NOTE: Step-detection algorithms for digitizing trajectories are generally less reliable when multiple molecular events overlap in time. Excluding polysome events from dwell time analysis is therefore recommended. For highly active translation systems that are enriched with polysome events and infrequently display monosome events, a mixture of labeled and unlabeled antibodies can be used to increase the chance of observing isolated translation events in single-molecule trajectories.

6.8.2. Fit the distribution to a log-normal function and use the fitted function to calculate the average dwell time.

NOTE: Calculating the mean directly by averaging the observed dwell times is not recommended because the dwell time distributions are typically skewed with long tails.

6.8.3. Determine the number of amino acids that are translated during the antibody binding dwell time by subtracting the sum of the epitope amino acid length and 35 (the average amino acid length of nascent peptide within the ribosome exit tunnel) from the total number of ORF codons.

6.8.4. To determine the average peptide synthesis rate, divide the number of translated amino acids by the average dwell time.

6.9. Optional: Calculation of the average first-round initiation time ($\langle t_{1\_I} \rangle$).

NOTE: Initiation and elongation conditions, such as the initiation site sequence context and the coding sequence, are generally preserved deliberately for studies of initiation kinetics. Therefore, the average first arrival time $\langle t_1 \rangle$ from step 6.7. can be used directly to calculate the change in first round initiation kinetics between different conditions. The following correction is only necessary for determining the actual value of first-round initiation time.

6.9.1. Divide the sum of the epitope length and 35 (the average amino acid length of nascent peptide within the ribosome exit tunnel) by the average peptide synthesis rate (from step 6.8.4.) to calculate the average peptide elongation time of this N-terminal region ($\langle t_{1\_tag} \rangle$).

6.9.2. As the first arrival time is the sum of the first-round initiation time and t_{1_tag}, subtract $\langle t_{1\_tag} \rangle$ from the average first arrival time $\langle t_1 \rangle$ to calculate the average first-round initiation time $\langle t_{1\_I} \rangle$: $\langle t_{1\_I} \rangle = \langle t_1 \rangle - \langle t_{1\_tag} \rangle$

7. Assay calibration

NOTE: Perform the following calibration steps when initially establishing the assay.

7.1. To examine the antibody binding specificity, perform the protocol steps in sections 4 and 5 separately for untagged and tagged mRNAs (**Figure 2**). The antibody binding levels in channels with these respective mRNAs represent the extent of nonspecific antibody binding to the detection surface and specific antibody binding to nascent peptide.

NOTE: The specific to nonspecific binding ratio is recommended to be >10 and may be increased with different surface passivation strategies, lower antibody concentration, or higher mRNA surface density.

7.2. To measure the rate of antibody binding, perform the protocol with an extra step between step 4 and step 5.

7.2.1. After step 4, incubate the channel with translation mixture that lacks antibody to pre-generate mRNA/ribosome/peptide complexes.

7.2.2. Then proceed to step 5 and flow antibody-supplemented translation mixture into the channel.

7.2.3. Quantify the average antibody binding rate to pre-generated nascent peptide with exponential fitting to the first arrival time histogram.

NOTE: Antibody binding to pre-generated peptide should be rapid, on the order of seconds, and should be faster than the translation kinetics. A higher antibody concentration may be used to increase the antibody binding rate.

7.3. Photostability of fluorophore-labeled antibody.

7.3.1. Prepare a slide according the protocol in step 2 but skip the PEGylation step. Assemble the flow chamber after the salinization step. The silane coating allows efficient nonspecific antibody binding to the detection surface.

7.3.2. Add the fluorescently-labeled antibodies into the channel to achieve single-molecule density of nonspecific antibody binding to the detection surface. Begin by adding fluorescently-labeled antibody that is highly diluted in T50 wash buffer and gradually increase the antibody concentration until the desired single-molecule density is achieved.

7.3.3. Image the detection surface until most of the antibody fluorescence is no longer detectable.

7.3.4. Plot the total number of visible antibodies over time to assess the rate of antibody fluorescence loss due to fluorophore photobleaching.

NOTE: Antibody labeling typically yields multiple fluorophores per antibody. Individual

antibodies remain detectable until all conjugated fluorophores photobleach.

REPRESENTATIVE RESULTS:

Following the protocol described enables the imaging of individual antibody interactions with nascent N-terminal-tagged polypeptides with single-molecule resolution during active cell-free translation of 3' end-tethered reporter mRNA (**Figure 1**). A minimal demonstration experiment is reported with the use of three synthetic mRNAs: *LUC* (encoding untagged luciferase), LUC_{FLAG} (encoding 3xFLAG-tagged luciferase), and *hp-*LUC_{FLAG} (LUC_{FLAG} with a stable stem-loop in the 5' leader region) (**Figure 2C**). The use of luciferase-encoding mRNA enables comparisons between single-molecule observations and bulk luminescence measurements. Integrity of 3' biotinylated mRNA was assessed by denaturing polyacrylamide gel electrophoresis (PAGE) and RNA staining. Good quality mRNA shows a single clean band and should not show additional faster migrating signals (**Figure 3A**). *Saccharomyces cerevisiae* translation extract was used here and prepared following a protocol that was previously described[30] and modified[15]. Bulk measurements of luciferase activity in cell-free translation reactions with the yeast extract and biotinylated LUC_{FLAG} mRNA that either lacks or contains an m^7G cap shows cap stimulation of LUC_{FLAG} mRNA translation (**Figure 3B**).

For single-molecule imaging, translation extract was supplemented with 67 nM of Cy3-labeled anti-FLAG antibody (Cy3-αFLAG). This antibody had a high labeling ratio of 2-7 dyes per antibody. The 532 nm laser was set to 10 μW at the objective. The laser incident angle was set to 71.5˚, which was greater than the critical angle of 63.8˚ for our set up. A low level of fluorescence was imaged from detection surfaces that contain mRNA but lack translation mix (**Figure 4A**). For channel dimensions of approximately 2 mm (width) x 50 μm (depth) x 24 mm (length), a flow delivery rate of 150 μl/min yielded a reagent exchange time of 3 – 4 s. Within 5 s of translation mix delivery, the background fluorescence level increases due to the diffusing fluorescent antibodies. Approximately 2 min after translation mix delivery to LUC_{FLAG} mRNA-containing channels, Cy3 spots began to appear in a field of view and continued to accumulate for ~30 min (**Figures 4B**). Nonspecific antibody binding to surface, measured using the 3xFLAG-lacking *LUC* mRNA (**Figure 2C**), remained at a very low level[15]. The signals from mRNA/ribosome/peptide-bound Cy3- αFLAG were clearly visible with the optimized laser incident angle but could be masked by a high fluorescence background with lower laser incident angles (**Figure 4C**).

To analyze Cy3-αFLAG binding events, the fluorescence intensities of selected Cy3-αFLAG spots (**Figure 5A**) were calculated frame by frame for the entire movie and then connected to form an intensity trajectory (**Figure 5B**). Raw trajectories can appear noisy and may require refinement with a non-linear forward-backward filter to reduce background noise[41]. Further refinement could be achieved using step-detection algorithms to digitize trajectories[42]. For all trajectories, a universal background fluorescence level increase appears during reagent exchange due to the diffusing fluorescent antibodies in the translation mix (**Figure 5B**). Antibody binding to a nascent polypeptide caused an instantaneous increase in fluorescence whereas antibody/polypeptide dissociation from mRNA causes an instantaneous fluorescence decrease (**Figure 5B**).

The dwell time of antibody binding can be used to measure the total decoding time of an open reading frame. The dwell time histogram for LUC_{FLAG} mRNA fits to a log-normal distribution (**Figure 6A**) and yielded a peptide synthesis rate of 2.5 ± 0.1 amino acids per second[15]. The first arrival time histogram fitted to a shifted (3-parameter) log-normal function (**Figure 6B**). The wide spread of the first arrival time histogram shows the high degree of heterogeneity in single mRNA translation activity. The histogram indicated that the first peptide synthesis event on single LUC_{FLAG} mRNA molecules could begin as early as 2 min, and as late as 20 min, after translation mix delivery (**Figure 6B**). Compared to translation with LUC_{FLAG} mRNA, the first arrival time histogram with *hp*-LUC_{FLAG} mRNA translation showed slower antibody binding (**Figure 7A**). Using bulk luminescence measurements from cell-free translation reactions with these same mRNAs, however, does not resolve differences in translation kinetics (**Figures 7B,C**). These results demonstrate the higher resolution of our method compared to bulk kinetic luciferase activity measurements for detecting small changes in initiation kinetics.

FIGURE AND TABLE LEGENDS

Figure 1: Protocol flow chart. Schematic representations of coverslip and slide preparation, single-molecule chamber assembly, TIRF imaging and data acquisition, and data analysis steps are shown. The TIRF imaging step includes schematic depictions of mRNA immobilization and translation in a flow channel. Detection surface components, fluorescently labeled antibody, and cell extract components are indicated.

Figure 2: mRNA designs for the single-molecule assay. (**A**) To adapt a bulk translation assay to the single-molecule assay, the DNA template of the bulk reporter ORF was modified with an N-terminal epitope tag sequence insertion to generate a tagged reporter-encoding ORF. ORF and N-terminal tag-coding regions are indicated. (**B**) mRNAs were 5′-m^{7}G capped to allow cap-dependent translation and 3′-biotinylated for their immobilization to single-molecule detection surface. 5′-m^{7}G cap and 3′-biotin are indicated on untagged and tagged ORF RNAs. (**C**) Luciferase-encoding mRNAs were used to demonstrate the single-molecule assay. *LUC* and LUC_{FLAG} mRNAs encode luciferase that lacks and contains an N-terminal 3xFLAG tag, respectively. *hp*-LUC_{FLAG} mRNA contains an additional insertion that introduces a hairpin secondary structure in the LUC_{FLAG} mRNA 5′-leader. The hairpin thermostability, 3′-poly(A) tail, and 3′-biotin are indicated. All three mRNAs included a 30 nt 3′-poly(A) tail for more efficient cap-dependent translation.

Figure 3: Single-molecule reporter mRNA integrity and bulk translation. (**A**) Representative denaturing PAGE imaging of single-molecule reporter mRNA. 5′-m^{7}G capped and 3′-biotinylated LUC_{FLAG} mRNA was loaded onto a denaturing 10% polyacrylamide gel next to an RNA ladder. (**B**) Single-molecule reporter mRNA preserved 5' cap-dependence in bulk cell-free translation reactions. 3′-biotinylated LUC_{FLAG} mRNA that either lacked (–cap) or contained (+ cap) a 5′-m^{7}G cap was translated in *S. cerevisiae* translation extract for 30 min at 25 ˚C. Luciferase activity was measured from two independent reactions and normalized to the activity with –cap mRNA,

which is arbitrarily set to 1.0. Standard deviations from mean values are indicated by error bars.

Figure 4: Imaging of detection surfaces containing immobilized mRNA. (**A**) Background fluorescence in the absence of translation mix. (**B**) Cy3 fluorescent spots in a field of view 30 min after the translation mix delivery and with an optimized laser incident angle. (**C**) Imaged field of view 30 min after translation mix delivery and with a low laser incident angle.

Figure 5: Image analysis. (**A**) Cy3 spots in a field of view without (left panel) or with (right panel) spot selection. (**B**) Example single-molecule trajectory for a selected Cy3 spot. The black arrow indicates the rise in background fluorescence due to diffusing antibody during translation mix delivery. The green arrow indicates the sudden increase in fluorescence intensity due to Cy3-αFLAG binding. The red arrow indicates the sudden decrease in fluorescence intensity due to Cy3-αFLAG/nascent peptide dissociation from mRNA. The dwell time of a Cy3-αFLAG binding event is indicated with a double-headed arrow. Raw, filtered, and digitized data are indicated.

Figure 6: Kinetic analysis of Cy3-αFLAG binding with *LUC_{FLAG}* mRNA translation. (**A**) The Cy3-αFLAG binding dwell time histogram fits to a log-normal distribution. (**B**) The Cy3-αFLAG binding first arrival time histogram fits to a shifted (3-parameter) log-normal function. Adapted from Wang et al.[15] with permission.

Figure 7: The single-molecule assay has a higher resolution for initiation kinetics than the bulk luminescence assay. (**A**) First arrival time histograms for Cy3-αFLAG binding with translation of *LUC_{FLAG}* and *hp-LUC_{FLAG}* mRNAs revealed slower initiation caused by a small hairpin structure in the mRNA 5′-leader. N = 10650 trajectories (*LUC_{FLAG}*), combined from 3 data sets and N = 4079 trajectories (*hp-LUC_{FLAG}*), combined from 2 data sets. (**B,C**) Bulk luciferase activity assay kinetic measurements did not resolve differences in initiation kinetics for *LUC_{FLAG}* (N = 9 data sets) and *hp-LUC_{FLAG}* (N = 6 data sets) mRNA translation. (**B**) Bulk luminescence kinetics. (**C**) Scatter plots of first round translation times determined by Gaussian fitting to the second derivative of the luminescence kinetics curves in (**B**), as described by Vassilenko *et al.*[46]. The red circles and bars in (**C**) represent the mean value and standard deviation of the calculated first round translation time, respectively. Adapted from Wang et al.[15] with permission.

DISCUSSION

In comparison to typical in vitro TIRF single-molecule experiments, single-molecule imaging with the assay described here is additionally complex due to the use of cell extract and a high concentration of fluorescently labeled antibody. Compared to the more common practice of one round of surface PEGylation, a second round of PEGylation (step 2) greatly reduces nonspecific antibody binding to detection surface[15]. The high concentration of diffusing fluorescent antibodies causes an extremely high fluorescent background that masks single-molecule detection of antibody binding. To reduce this fluorescent background, the laser incident angle is increased well above the critical angle (step 3.4.). Antibody detection is also diminished by excessive fluorophore instability, which can limit the capability to quantify dwell time. When encountering this problem, replace the fluorophore with a more photostable fluorophore, such as the ones conjugated to a triplet-state quencher[47], or lower the laser

illumination intensity. Although oxygen scavenging systems are commonly used in in vitro single-molecule experiments to suppress fluorophore photobleaching[48,49], the assay described here can provide a very generous detection window without implementing any oxygen scavenging systems[15]. Furthermore, oxygen scavenging systems can greatly reduce eukaryotic cell-free translation efficiency. Therefore, oxygen scavenging systems should be carefully evaluated prior to their use with this assay.

It is important to point out that small variations in reagent preparation are detected by the assay due to its single-molecule resolution. For example, replicate translation extract preparations can display different activities that may or may not be detectable by bulk methods. Furthermore, freeze-thaw cycles of translation extract and other reagents can rapidly impair translation activity. We recommend doing small-scale pilot experiments with readily accessible material to test conditions before planning for a systematic study. For a systematic study, large-scale preparations of translation reagents, single-use aliquots for freeze/thaw-sensitive reagents, and consistency in performing protocol steps are recommended. Translation extract that is flash frozen in liquid nitrogen and stored at −80 ˚C shows minimal activity loss for at least two years. Application of these measures can effectively suppress experimental variations and increase the robustness of the single-molecule assay.

As this method combines existing bulk cell-free translation systems and in vitro single-molecule imaging techniques, troubleshooting of generic problems in these two areas are not discussed here. Examples of such generic issues include low quality preparations of reporter mRNA or PEGylated coverslip and low translation activity of cell extract. Here, we will focus on issues specific for this method. In addition to the several technical issues that have been discussed in the protocol, another potential problem may be low or no antibody binding in the flow channel for a translation condition that is expected to have good activity. There are several possibilities to troubleshoot. The efficiency of biotinylated mRNA immobilization to the detection surface can be assessed by annealing complementary and fluorophore-conjugated DNA oligomers to the immobilized mRNA and imaging the fluorescent DNA:RNA duplexes. The quality of the translation mix and biotinylated reporter mRNAs can be checked by running the bulk translation assay. Furthermore, after carrying out a translation reaction in an mRNA-immobilized flow channel, the translation reaction solution can be pipetted out of the channel and used in a reporter activity assay to confirm the occurrence of in-channel translation. If necessary, an excessively high mRNA surface density can be used for the in-channel translation reaction to allow easier detection by the reporter activity assay.

The major limitation of this assay is its resolution for initiation kinetics. In this assay, the direct experimental output, first arrival time, contains both the first-round initiation time and the peptide elongation time for translating the epitope and 35 additional codons. Although the contribution of the peptide elongation time can be corrected (step 6.9.), this assay consequently is most sensitive for measuring initiation kinetics that occur on the order of minutes, which appears to be a generic property of cap-dependent initiation[15]. Experimentally, it is easy to adapt this assay to study other initiation mechanisms. However, if an initiation mechanism occurs significantly fast on the order of seconds, this assay is unlikely to resolve the

initiation kinetics.

The single-molecule approach described here combines single-molecule imaging and extract-based translation to enable measurements of individual cap-dependent translation events in real-time and during active cell-free translation. The assay allows easy transitioning from a bulk translation assay to a single-molecule assay, while preserving the bulk translation kinetics. Thus, single-molecule kinetic observations can be interpreted in direct reference to corresponding bulk results. Previous methods, including recently developed in vivo approaches[11-14], lack the resolution for kinetic measurements of individual translation initiation events and require assumptions of translation mechanisms to extract initiation time averages from experimental observables. The single-molecule method presented here provides the first hypothesis-free approach for quantifying the average initiation time of active cap-dependent translation. Furthermore, although bulk kinetic measurements with a luminescence assay have been utilized to provide the most quantitative and systematic bulk characterizations of cap-dependent translation kinetics to date[46,50], the single-molecule assay described here measures average initiation kinetic changes with greater sensitivity than the bulk assay (**Figure 7**). In addition, the single-molecule data preserves single mRNA translation stochasticity and heterogeneity, properties that are averaged out in bulk measurements. The single-molecule resolution of translation kinetics can be utilized for systematic kinetic analyses to reveal insights of translation mechanisms unattainable with other methods.

This assay is compatible with existing biochemical and genetic approaches that are commonly used for translation studies. For example, the translational function of a specific factor can be studied by generating factor-depleted extract and supplementing it with wild-type or mutant factor. In addition, by supplementing fluorescently labeled factor, studies can potentially investigate the kinetic relationship between factor binding and the progression of translation. With the use of two distinct epitope/antibody pairs, this protocol could potentially be expanded from a one-color assay to a two-color assay that enables simultaneous detection of two distinct coding sequences. This adaptation would allow tracking the translation of different reading frames and could be applied to frameshifting and start site selection studies. Alternatively, a two-color system could be used to detect antibody interactions with tagged polypeptides encoded by upstream and downstream open reading frames to monitor both upstream and downstream translation events on individual mRNAs. These expansions can enable a wide range of mechanistic studies that investigate cap-dependent translation and its regulation.

ACKNOWLEDGMENTS

This work was supported by the National Institutes of Health [R01GM121847]; the Memorial Sloan Kettering Cancer Center (MSKCC) Support Grant/Core Grant (P30 CA008748); and MSKCC Functional Genomics Initiative.

DISCLOSURES

The authors have nothing to disclose.

REFERENCES

1. Hinnebusch, A. G. The scanning mechanism of eukaryotic translation initiation. *Annual Review of Biochemistry.* **83**, 779–812 (2014).
2. Gebauer, F., Hentze, M.W. Molecular mechanisms of translational control. *Nature Reviews Molecular Cell Biology.* **5**, 827–835 (2004).
3. Jackson, R. J., Hellen, C. U., Pestova, T. V. The mechanism of eukaryotic translation initiation and principles of its regulation. *Nature Reviews Molecular Cell Biology.* **11**, 113–127 (2010).
4. Silvera, D., Formenti, S. C., Schneider, R. J. Translational control in cancer. *Nature Reviews Cancer.* **10**, 254–266 (2010).
5. Saini, A. K., Nanda, J. S., Lorsch, J. R., Hinnebusch, A. G. Regulatory elements in eIF1A control the fidelity of start codon selection by modulating tRNA(i)(Met) binding to the ribosome. *Genes and Development.* **24**, 97–110 (2010).
6. Algire, M. A. et al. Development and characterization of a reconstituted yeast translation initiation system. *RNA.* **8**, 382–397 (2002).
7. Amrani, N., Ghosh, S., Mangus, D. A., Jacobson, A. Translation factors promote the formation of two states of the closed-loop mRNP. *Nature.* **453**, 1276–1280 (2008).
8. Pisarev, A. V., Unbehaun, A., Hellen, C. U., Pestova, T.V. Assembly and analysis of eukaryotic translation initiation complexes. *Methods in Enzymology.* **430**, 147–177 (2007).
9. Hinnebusch, A. G. Structural insights into the mechanism of scanning and start codon recognition in eukaryotic translation initiation. *Trends in Biochemical Sciences.* **42**, 589–611 (2017).
10. Iwasaki, S., Ingolia, N. T. The growing toolbox for protein synthesis studies. *Trends in Biochemical Sciences.* **42**, 612–624 (2017).
11. Morisaki, T. et al. Real-time quantification of single RNA translation dynamics in living cells. *Science.* **352**, 1425–1429 (2016).
12. Wang, C., Han, B., Zhou, R. & Zhuang, X. Real-time imaging of translation on single mRNA transcripts in live cells. *Cell.* **165**, 990–1001 (2016).
13. Wu, B., Eliscovich, C., Yoon, Y. J., Singer, R.H. Translation dynamics of single mRNAs in live cells and neurons. *Science.* **352**, 1430–1435 (2016).
14. Yan, X., Hoek, T. A., Vale, R. D., Tanenbaum, M. E. Dynamics of translation of single mRNA molecules in vivo. *Cell.* **165**, 976–989 (2016).
15. Wang, H., Sun, L., Gaba, A., Qu, X. An in vitro single-molecule assay for eukaryotic cap-dependent translation initiation kinetics. *Nucleic Acids Research.* **48**, e6 (2020).
16. Aitken, C. E., Lorsch, J.R. A mechanistic overview of translation initiation in eukaryotes. *Nature Structural & Molecular Biology.* **19**, 568–576 (2012).
17. Anderson, C. W., Straus, J. W., Dudock, B.S. Preparation of a cell-free protein-synthesizing system from wheat germ. *Methods in Enzymology* **101**, 635–644 (1983).
18. Erickson, A. H., Blobel, G. Cell-free translation of messenger RNA in a wheat germ system. *Methods in Enzymology.* **96**, 38–50 (1983).
19. Iizuka, N., Najita, L., Franzusoff, A., Sarnow, P. Cap-dependent and cap-independent translation by internal initiation of mRNAs in cell extracts prepared from Saccharomyces cerevisiae. *Molecular and Cellular Biology.* **14**, 7322–7330 (1994).
20. Iizuka, N., Sarnow, P. Translation-competent extracts from Saccharomyces cerevisiae:

792 effects of L-A RNA, 5' cap, and 3' poly(A) tail on translational efficiency of mRNAs. *Methods.* **11**,
793 353–360 (1997).
794 21. Jackson, R. J., Hunt, T. Preparation and use of nuclease-treated rabbit reticulocyte
795 lysates for the translation of eukaryotic messenger RNA. *Methods in Enzymology.* **96**, 50–74
796 (1983).
797 22. Sachs, M. S. et al. Toeprint analysis of the positioning of translation apparatus
798 components at initiation and termination codons of fungal mRNAs. *Methods.* **26**, 105–114
799 (2002).
800 23. Tarun, S. Z., Jr., Sachs, A. B. A common function for mRNA 5' and 3' ends in translation
801 initiation in yeast. *Genes and Development.* **9**, 2997–3007 (1995).
802 24. Wang, Z., Sachs, M.S. Ribosome stalling is responsible for arginine-specific translational
803 attenuation in Neurospora crassa. *Molecular and Cellular Biology.* **17**, 4904–4913 (1997).
804 25. Wang, Z., Sachs, M.S. Arginine-specific regulation mediated by the Neurospora crassa
805 arg-2 upstream open reading frame in a homologous, cell-free in vitro translation system.
806 *Journal of Biological Chemistry.* **272**, 255–261 (1997).
807 26. Fedyukina, D. V., Cavagnero, S. Protein folding at the exit tunnel. *Annual Review of*
808 *Biophysics.* **40**, 337–359 (2011).
809 27. Jha, S., Komar, A.A. Birth, life and death of nascent polypeptide chains. *Biotechnology*
810 *Journal.* **6**, 623–640 (2011).
811 28. Gregorio, N. E., Levine, M. Z., Oza, J. P. A user's guide to cell-free protein synthesis.
812 *Methods and Protocols.* **2**, 24 (2019).
813 29. Zhovmer, A., Qu, X. Proximal disruptor aided ligation (ProDAL) of kilobase-long RNAs.
814 *RNA Biology.* **13**, 613–621 (2016).
815 30. Wu, C., Sachs, M. S. Preparation of a Saccharomyces cerevisiae cell-free extract for in
816 vitro translation. *Methods in Enzymology.* **539**, 17–28 (2014).
817 31. Zhao, R., Rueda, D. RNA folding dynamics by single-molecule fluorescence resonance
818 energy transfer. *Methods.* **49**, 112–117 (2009).
819 32. Chandradoss, S. D. et al. Surface passivation for single-molecule protein studies. *Journal*
820 *of Visualized Experiments.* (86) 50549 (2014).
821 33. Deindl, S., Zhuang, X. Monitoring conformational dynamics with single-molecule
822 fluorescence energy transfer: applications in nucleosome remodeling. *Methods in Enzymology.*
823 **513**, 59–86 (2012).
824 34. Greene, E. C., Wind, S., Fazio, T., Gorman, J., Visnapuu, M. L. DNA curtains for high-
825 throughput single-molecule optical imaging. *Methods in Enzymology.* **472**, 293–315 (2010).
826 35. Gaba, A., Wang, Z., Krishnamoorthy, T., Hinnebusch, A. G., Sachs, M.S. Physical evidence
827 for distinct mechanisms of translational control by upstream open reading frames. *The EMBO*
828 *Journal.* **20**, 6453–6463 (2001).
829 36. Schaffer, B., Grogger, W., Kothleitner, G. Automated spatial drift correction for EFTEM
830 image series. *Ultramicroscopy.* **102**, 27–36 (2004).
831 37. Wang, Y. et al. Localization events-based sample drift correction for localization
832 microscopy with redundant cross-correlation algorithm. *Optics Express.* **22**, 15982–15991
833 (2014).
834 38. Sugar, J. D., Cummings, A. W., Jacobs, B. W., Robinson, B. D. A free Matlab script for
835 spacial drift correction. *Microscopy Today.* **22**, 40–47 (2014).

39. Chenouard, N. et al. Objective comparison of particle tracking methods. *Nature Methods.* **11**, 281–289 (2014).
40. Meijering, E., Dzyubachyk, O., Smal, I. Methods for cell and particle tracking. *Methods in Enzymology.* **504**, 183–200 (2012).
41. Chung, S. H., Kennedy, R. A. Forward-backward non-linear filtering technique for extracting small biological signals from noise. *Journal of Neuroscience Methods.* **40**, 71–86 (1991).
42. Ensign, D. L., Pande, V.S. Bayesian detection of intensity changes in single molecule and molecular dynamics trajectories. *Journal of Physical Chemistry B.* **114**, 280–292 (2010).
43. Blanco, M., Walter, N. G. Analysis of complex single-molecule FRET time trajectories. *Methods in Enzymology.* **472**, 153–178 (2010).
44. Shuang, B. et al. Fast step transition and state identification (STaSI) for discrete single-molecule data analysis. *The Journal of Physical Chemistry Letters.* **5**, 3157–3161 (2014).
45. White, D. S., Goldschen-Ohm, M. P., Goldsmith, R. H., Chanda, B. Top-down machine learning approach for high-throughput single-molecule analysis. *Elife.* **9**, e53357 (2020).
46. Vassilenko, K. S., Alekhina, O. M., Dmitriev, S. E., Shatsky, I. N., Spirin, A. S. Unidirectional constant rate motion of the ribosomal scanning particle during eukaryotic translation initiation. *Nucleic Acids Research.* **39**, 5555–5567 (2011).
47. Zheng, Q. et al. Ultra-stable organic fluorophores for single-molecule research. *Chemical Society Review.* **43**, 1044–1056 (2014).
48. Aitken, C. E., Marshall, R. A., Puglisi, J.D. An oxygen scavenging system for improvement of dye stability in single-molecule fluorescence experiments. *Biophysical Journal.* **94**, 1826–1835 (2008).
49. Shi, X., Lim, J., Ha, T. Acidification of the oxygen scavenging system in single-molecule fluorescence studies: in situ sensing with a ratiometric dual-emission probe. *Analytical Chemistry.* **82**, 6132–6138 (2010).
50. Berthelot, K., Muldoon, M., Rajkowitsch, L., Hughes, J., McCarthy, J. E. Dynamics and processivity of 40S ribosome scanning on mRNA in yeast. *Molecular Microbiology.* **51**, 987–1001 (2004).

Figure 1

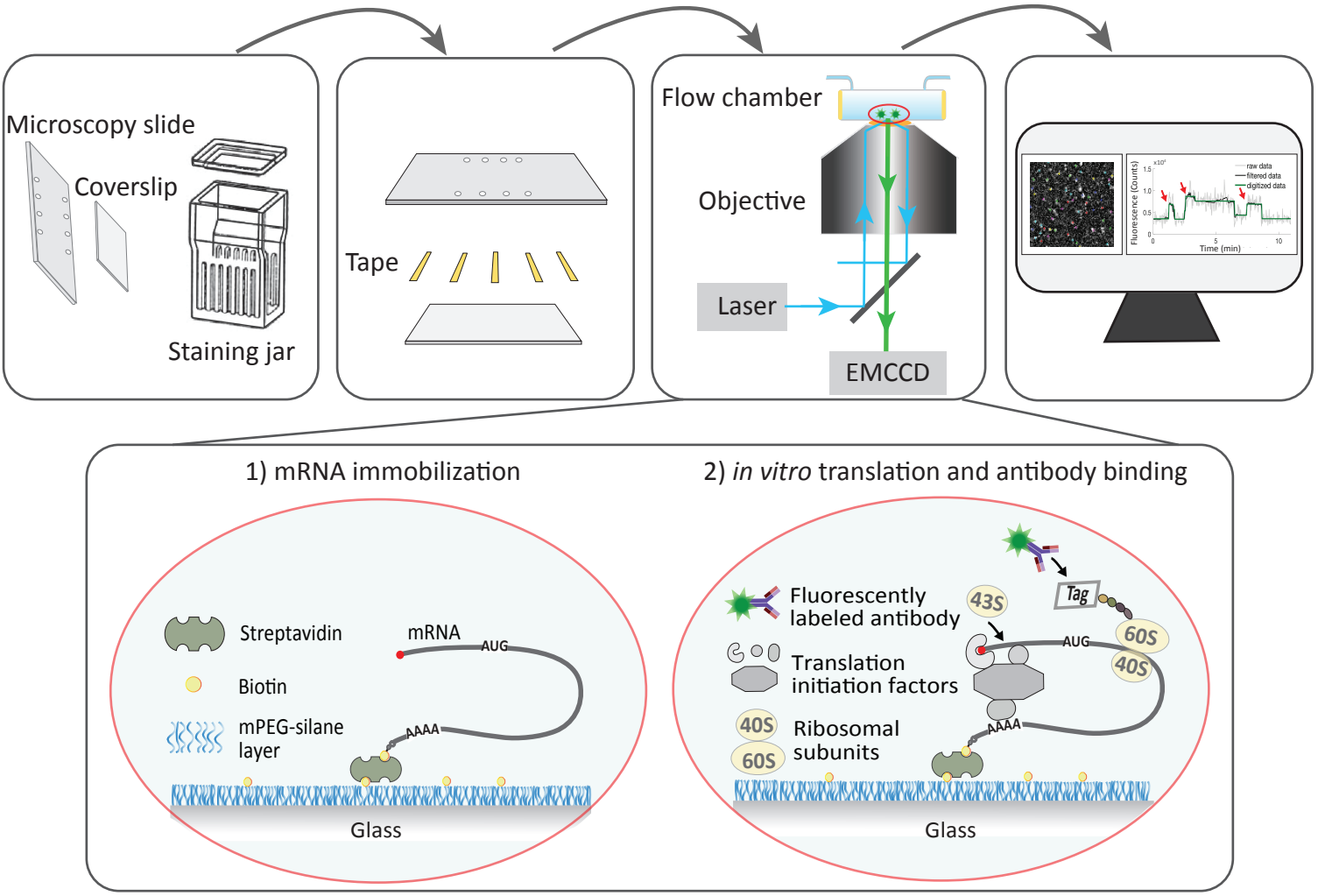

Figure 2

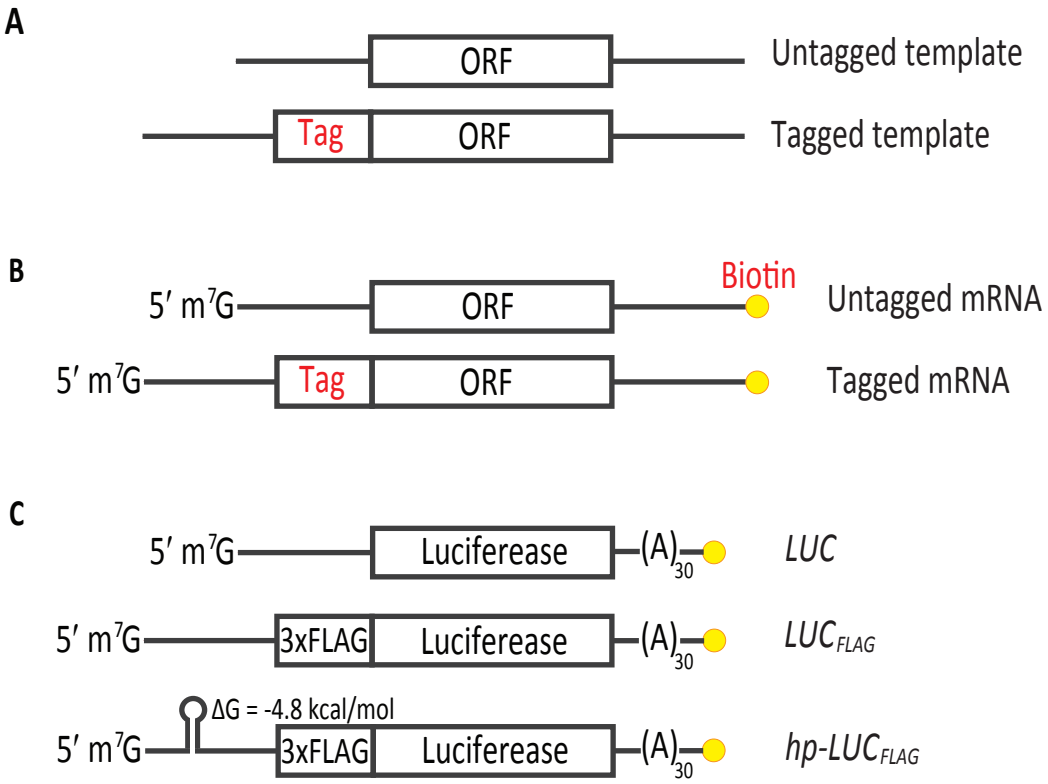

Figure 3

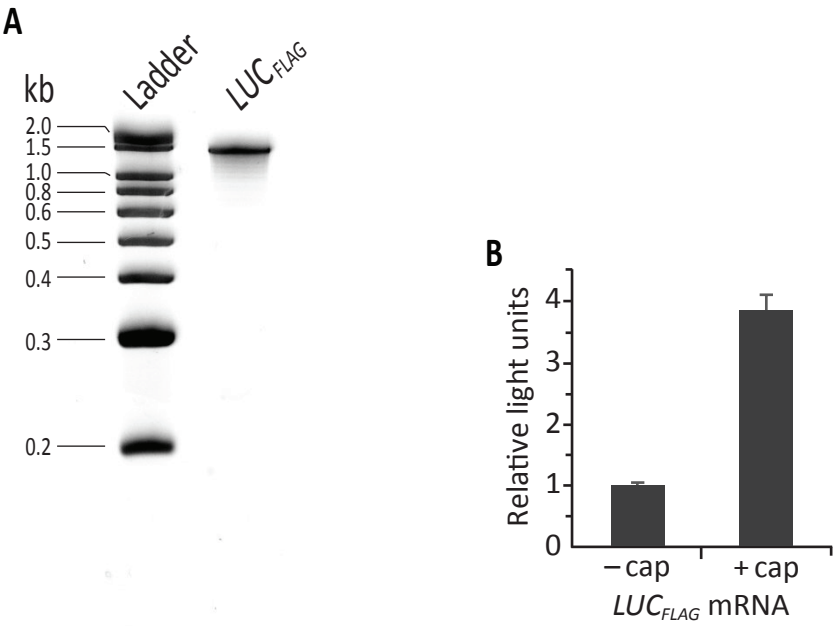

Figure 4

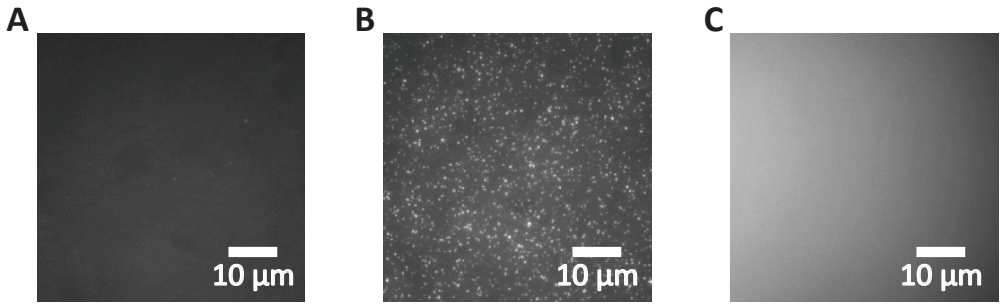

Figure 5

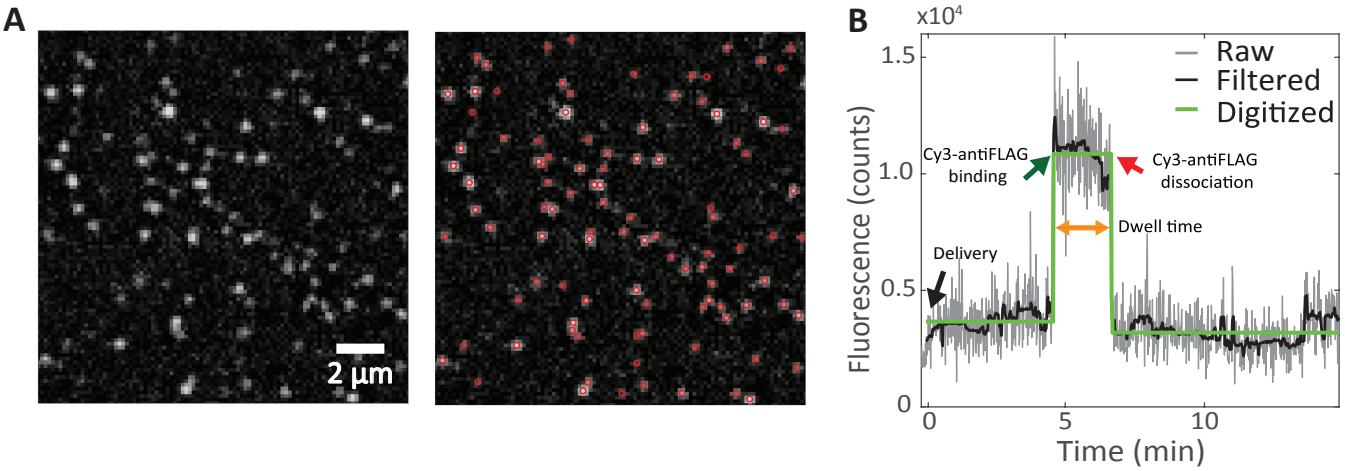

Figure 6

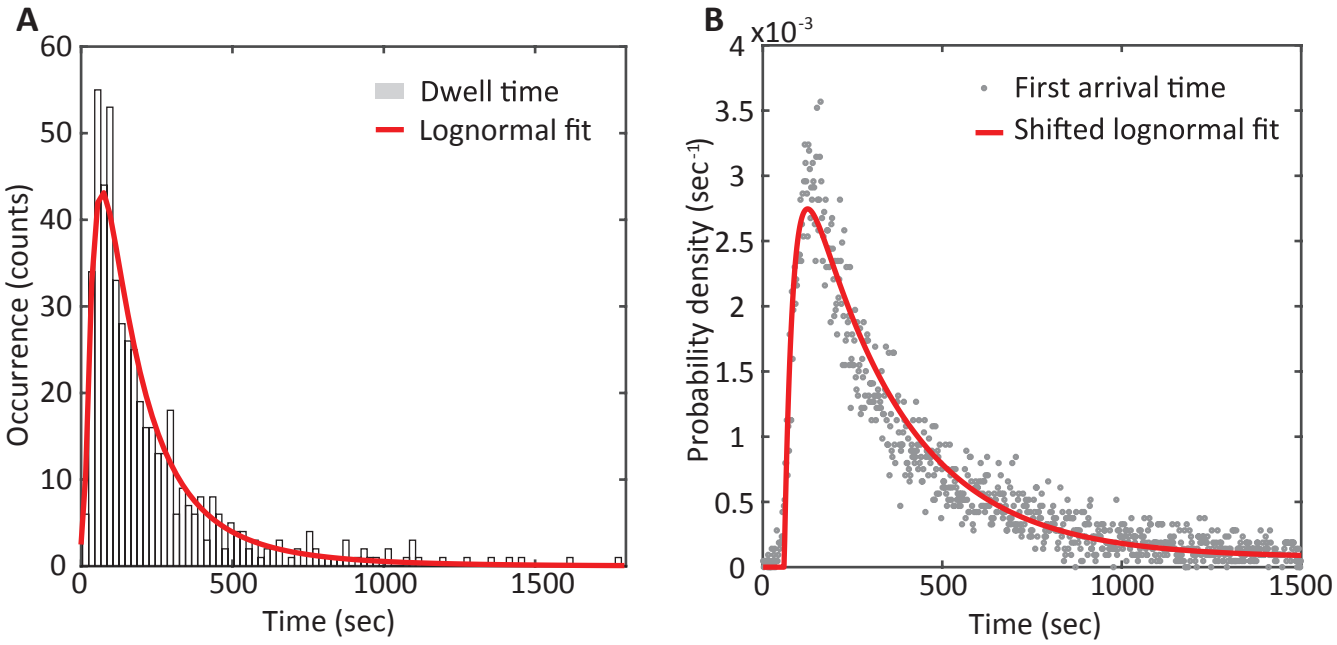

Figure 7

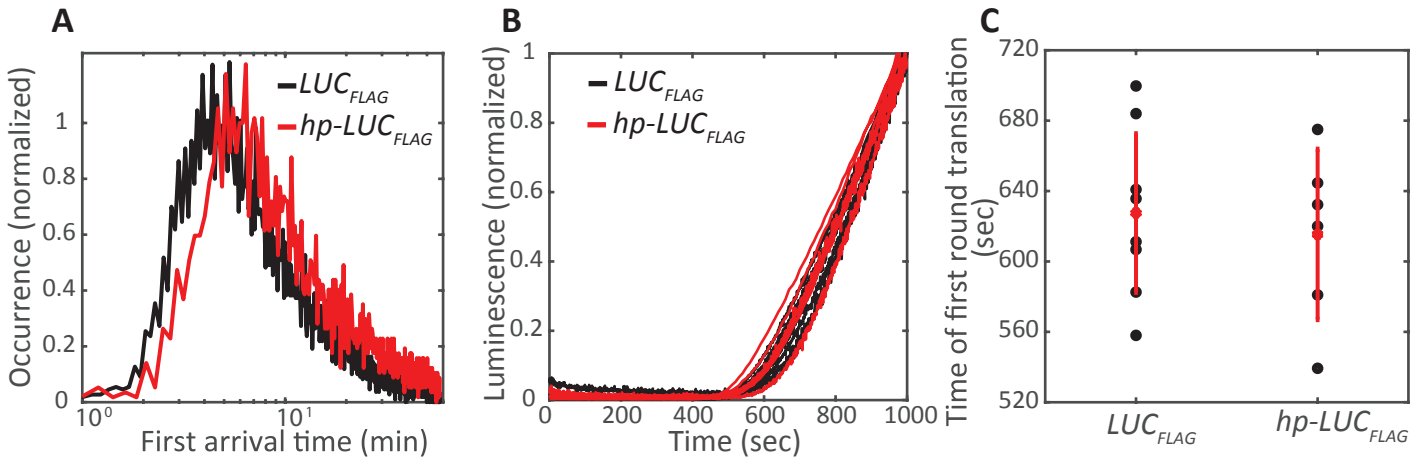

Name of Material/Equipment

100X oil objective, N.A. 1.49
Acryamide/bis (40%, 19:1)
Alkaline liquid detergent
Aminosilane (N-(2-Aminoethyl)-3-Aminopropyltrime
Andor ixon Ultra DU 897V EMCCD
Andor *Solis* software
Band-pass filter
Band-pass filter
Biotin-PEG-SVA
Coenzyme A free acid
Coolterm software
Desktop computer
Dichroic mirror
Direct-zol RNA microprep 50RNX
Dual-Luciferase Reporter Assay System
Epoxy
Firefly luciferin D-Luciferin free acid
Glacial acetic acid
Hydrogen perioxide
Immersion oil
Luciferase Assay System
MEGASCRIPT T7 Transcription Kit
Methanol
Microscope
Microscope slide
Monoclonal anti-FLAG M2-Cy3
mPEG-SVA
MS(PEG)4
NaCl (5M)
No 1.5 microscope Cover glass
Olympus Laser, 532nm 100mM

Olympus *TirfCtrl* software
Optical table
Phenol chloroform isoamyl alcohol mix
Pierce RNA 3' End Biotinylation Kit
Potassium hydroxide pellets
Prior motorized XY translation stage
Prior *PriorTest* software
Recombinant RNasin RNase Inhibitor
Stage top Incubator
Staining jar
Streptavidin
Sulfuric acid
SYBR green II
Syringe
Syringe pump
Tris (1M), pH = 7.0
Ultrasonic Bath
Urea
Vaccinia Capping system
Zymo-Spin IC Columns

Company	**Catalog Number**
Olympus	UAPON 100XOTIRF
Bio-Rad	161-0144
Decon	5332
UCT Specialties, LLC	A0700
Andor	DU-897U-CSO-#BV
Andor	
Chroma	532/640/25
Chroma	NF03-405/488/532/635E-25
Laysan Bio Inc	Biotin-PEG-SVA
Prolume	309-250
Dell	
Semrock	R405/488/532/635
Fisher Scientific	NC1139450
Promega	E1910
Devcon	14250
Prolume	306-250
Fisher Scientific	BP1185500
Sigma-Aldrich	216763-500ML
Olympus	Z-81226A
Promega	E1500
Thermo fisher	AM1334
Fisher Scientific	MMX04751
Olympus	IX83
Thermo Scientific	3048
Sigma-Aldrich	A9594
Laysan Bio Inc	mPEG-SVA-5000
Thermo Scientific	22341
Thermo Scientific	AM9760G
Fisherband	12-544-C
Olympus digital Laser system	CMR-LAS 532nm 100mW

Olympus	
TMC vibration control	63-563
Sigma-Aldrich	77617-100ml
Thermo Scientific	20160
Sigma-Aldrich	P1767-500G
Prior	PS3J100
Prior	
Promega	N2515
In vivo scientific (world precisic	98710-1
Fisher Scientific	08-817
Thermo Scientific	43-4301
Fisher Scientific	A300212
Fisher Scientific	S7564
Hamilton	1725RN
Harvard apparatus	55-3333
Thermo Scientific	AM9850G
Branson	CPX1800H
Sigma-Aldrich	U5378-500G
New England Biolabs	M2080S
Zymo Research	C1004

Comments/Description

For controlling the Andor EMCCD

For controlling the syringe pump
For controlling the microscope, camera, stage, and pump.

Low auto-fluorescence

For controlling the laser intensity and incident angle
With vibration isolation

For controlling the Prior motorized stage

With a custom built acrylic cage

Xiaohui Qu, Ph.D.
Assistant Member
Molecular Biology
Sloan-Kettering Institute

Dear Editor,

Thank you for your suggestions to improve the clarity of our manuscript. We have revised the manuscript following the editorial comments and our previous phone discussion.

We appreciate your consideration of our revised manuscript.

Sincerely,

Xiaohui Qu, Ph.D

Memorial Sloan Kettering Cancer Center
1275 York Avenue, Box 191, New York, NY 10065
Office: 212.639.2020 • Cell: 646.771.6815
E-mail: qux@mskcc.org

Click here to access/download;Supplemental File (Figures, Permissions_Oxf_NAR_copyright.pdf

Copyright Licence

Upon receipt of accepted manuscripts at Oxford Journals authors will be invited to complete an online copyright licence to publish form. If the form has not been received by the time we receive author corrections, publication of your manuscript may be delayed.

As part of the licence agreement, authors may use their own material in other publications provided that the Journal is acknowledged as the original place of publication and Oxford University Press as the Publisher. Information about the New Creative Commons licence.

Please note that by submitting an article for publication you confirm that you are the corresponding/submitting author and that Oxford University Press ("OUP") may retain your email address for the purpose of communicating with you about the article. You agree to notify OUP immediately if your details change. If your article is accepted for publication OUP will contact you using the email address you have used in the registration process. Please note that OUP does not retain copies of rejected articles.